

Endothermic reactions of uranium ions with N₂, D₂, and CD₄

P. B. Armentrout, R. V. Hodges, and J. L. Beauchamp*

Arthur Amos Noyes Laboratory of Chemical Physics, California Institute of Technology, Pasadena, California 91125

(Received 10 January 1977)

An ion beam apparatus is employed to study the reactions of uranium ions with N₂, D₂, and CD₄ at laboratory energies up to 335 eV. The endothermic reaction of U⁺ with nitrogen leads to the product UN⁺ for which a bond dissociation energy $D(\text{UN}^+) = 4.7 \pm 0.2$ eV is determined, corresponding to $\Delta H_f(\text{UN}^+) = 272 \pm 7$ kcal/mole. Endothermic reactions of U⁺ with D₂ and CD₄ lead to formation of UD⁺ with $D(\text{UD}^+) = 2.9 \pm 0.1$ eV and $\Delta H_f(\text{UD}^+) = 254 \pm 6$ kcal/mole. The dependence of experimental reaction cross sections on relative kinetic energy is discussed in terms of simple models for reaction. The proton affinity of uranium is determined, P.A.(U) = 238 ± 5 kcal/mole, and this exceptionally high value is compared to other atomic and molecular base strengths.

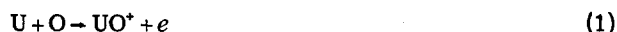
I. INTRODUCTION

The assessment of new technology for isotope separation has revived an interest in the spectroscopy, properties, and reactions of uranium and its compounds. Newer methods which have been demonstrated include the use of lasers to selectively excite a particular uranium isotope with subsequent chemical or physical separation.^{1,2} In addition, several new electromagnetic and electrostatic schemes for separation of ions containing uranium appear promising. These include ion cyclotron resonance,^{3,4} quadrupole mass filters,⁵ and energy separation methods based on high energy collision induced dissociation reactions.⁶ The successful development and implementation at practical levels of many of these processes requires a knowledge of the gas phase reactivity, heats of formation, and bond dissociation energies of neutral and ionic uranium compounds. For example, a molecule which reacts only with an excited or ionized uranium species could be used to chemically separate the selectively excited isotope in laser schemes. In another area where gas phase thermochemical data are useful, Fite and co-workers^{7(a)} have pointed out that molecular ion products of associative ionization reactions involving ground state uranium atoms at thermal energies are energetically forbidden to become neutralized by dissociative recombination with electrons. This affords the possibility of producing high density plasmas suitable for use in electromagnetic and electrostatic separation methods.

Presently, most of the thermodynamic data available concern uranium containing solids.⁶ Knudsen cell studies have yielded gas phase data for uranium oxides,⁹ sulphides,¹⁰ fluorides,¹¹ nitrides,^{12(a)} carbides,^{12(b)} and borides.^{12(c)} Further information regarding the gas phase thermodynamics and reactions of uranium fluorides has been obtained by Compton¹³ using mass spectrometric methods including a detailed analysis of energetic alkali atom reactions, by Beauchamp¹⁴ using the techniques of ion cyclotron resonance spectroscopy, and by McAskill¹⁵ using high pressure mass spectrometry.

Fite has characterized the reactions of uranium atoms with oxygen atoms^{7(c)} and various molecules using ther-

mal beams.⁷ He finds, for example, that the associative ionization process



occurs with a cross section of 16 Å² at thermal energies. Figure 1 shows a simplified diagram illustrating the energetics of the generalized reaction



The relationship

$$D(\text{UA}) + \text{I.P.}(\text{U}) = D(\text{UA}^+) + \text{I.P.}(\text{UA}), \quad (3)$$

where $D(\text{X})$ and $\text{I.P.}(\text{X})$ refer to the bond dissociation energy and ionization potential, respectively, of species X, follows directly from Fig. 1. For process (2) to be exothermic at thermal energies, it is required that $D(\text{UA}) \geq \text{I.P.}(\text{UA})$, which in turn implies that $D(\text{UA}^+) \geq \text{I.P.}(\text{U})$. The energetics of the possible reactions of uranium with molecular species, Eqs. (4)–(7), can be similarly treated:

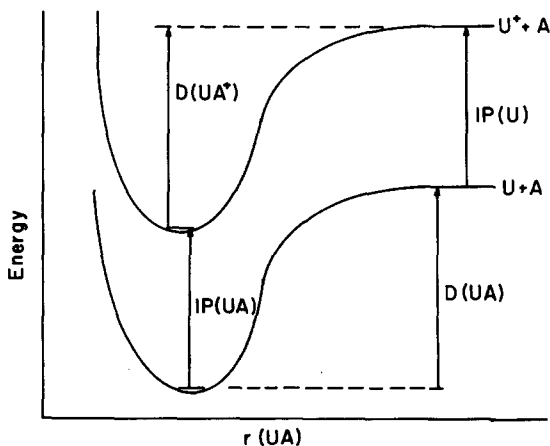
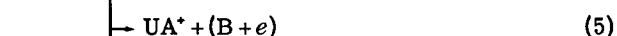


FIG. 1. Simplified energy diagram for the generalized associative ionization reaction (2). Illustrated are conditions for an exothermic reaction [$D(\text{UA}) > \text{IP}(\text{UA})$].

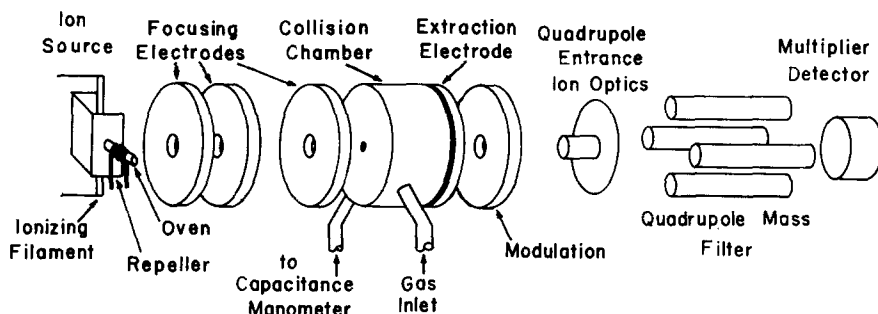


FIG. 2. Schematic drawing of the ion beam apparatus and uranium ion source.

Wexler and co-workers¹⁶ have characterized the chemi-ionization reactions of uranium atoms with oxygen molecules at energies up to 70 eV, considerably extending Fite's earlier investigation using thermal beams.^{7(c)} At low energies the only product ion is UO_2^+ [process (6)]. As the energy is increased UO^+ formed in process (5) begins to predominate. At the highest energies U^+ becomes the major product [process (4)].

There appear to be only two previous investigations of the reactions of atomic uranium ions. Moreland, Rokop, and Stevens¹⁷ observed the formation of UH^+ and UD^+ from reactions with H_2 , D_2 , H_2O , D_2O , and H_2S . However, their quantitative characterization of these species suffers from ill-defined reaction conditions in their experiment. The exothermic reaction



has been studied by Johnsen and Biondi.¹⁸ They were unable, however, to find evidence for a similar reaction with nitrogen



with lab energies ranging to 5 eV.

In the present investigation, a beam of uranium ions of well defined kinetic energy is allowed to interact with a gas in the fieldfree region of a collision chamber. Product abundances are analyzed as a function of pressure of the target gas to yield reaction cross sections and as a function of relative kinetic energy to yield thermochemical data. Specifically, the reaction



where AB is N_2 , D_2 , and CD_4 , is characterized and discussed.

II. EXPERIMENTAL

The ion beam apparatus has been previously described¹⁹ and is shown schematically in Fig. 2. Ions from a surface ionization source are focussed into a collision chamber containing the reactant gas. Energy of the ion beam is determined by the difference in potential between the chamber and the center of the filament, the latter being determined using a resistive divider. The spread in ion energies is estimated to be ≤ 0.3 eV with a comparable uncertainty in the calibration of the energy scale. Due to center of mass to laboratory conversion factors and the large Doppler spread in relative kinetic energies, this introduces

negligible uncertainties into the determined endothermic reaction thresholds. Product ions scattered in the forward direction are detected using a quadrupole mass spectrometer. The entrance and exit apertures of the chamber are 1.0 and 1.5 mm in diameter, respectively. The reaction path length is 5 mm. The collision chamber is designed to efficiently extract low energy product ions using a small extraction field.²⁰ In the present experiments the collision chamber is maintained as a field-free interaction region. Use of an extraction field did not alter product ion yields. This verifies calculations²¹ which show that the large mass of the ionic reactants and products compared to the neutrals involved result in product ion collection efficiencies of near 100% for the reactions studied. Resolution of the quadrupole is sufficient to easily resolve UD^+ (but not UH^+) from U^+ . This dictated the use of D_2 and CD_4 as neutral reactants.

The uranium ion source is comprised of a tubular stainless steel oven attached to the side of a U-shaped repeller plate. The oven is loaded from the rear with solid UF_4 and sealed with a set screw. The rhenium filament used for surface ionization (dimensions $0.030 \times 0.762 \times 11.9$ mm) is resistively heated with a current which is typically 4.5 A. This generates sufficient heat to vaporize the UF_4 which effuses through a hole, 0.50 mm in diameter. Although it was unnecessary in the present experiment, the capacity to heat the oven independently is provided by heating wire. The UF_4 vapor undergoes dissociation and surface ionization on the filament.²² This provides an ion beam consisting of U^+ and UF^+ . A typical ratio of UF^+ to U^+ was 1:100 with small variations depending on filament temperature. Ion beam currents in the range of 10^{-9} – 10^{-12} A were sufficient for the present experiments. The lifetime of the source, usually 50 h, is limited by filament failure.

We estimate the filament temperature to be 2300 °K. Uranium ions have several low lying states²³ which can be thermally populated at the temperature of the surface ionization source. No attempt is made in the present work to account for the presence of excited states. It is expected that the principal effect would be a low energy tail in the threshold region for endothermic reactions. The oven temperature is 700 °K (as measured by a chromel–constantan thermocouple) and the collision chamber is at 400 °K (as measured by a thermistor) under normal operating conditions. Since the capacitance manometer head is at room temperature, a thermal transpiration correction²⁴ was applied to the measured pressure.

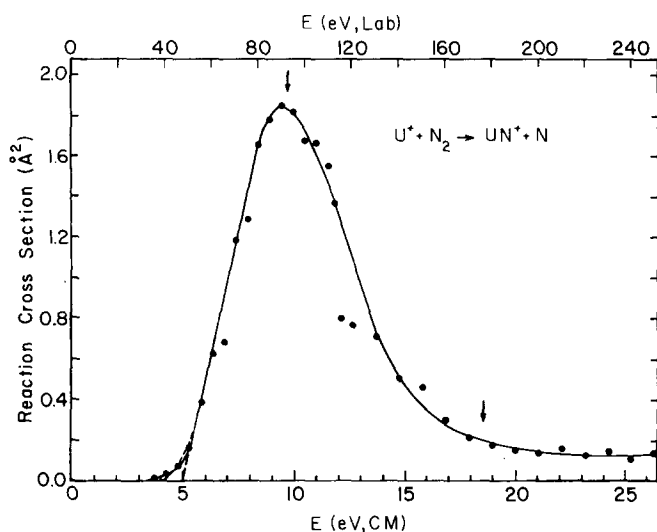


FIG. 3. Variation of experimental cross section with relative kinetic energy in the center of mass frame (lower scale) and the laboratory frame (upper scale) for Reaction (9). The solid curve is an approximate fit to the experimental points. The straight dashed line (—) is a linear extrapolation of the data in the threshold region. The curved dashed line (---) is the threshold behavior predicted by Chantry's analysis at a temperature of 400°K. The arrow at 9.8 eV indicates the threshold for the product channel $U^* + N + N$. The arrow at 18.6 eV indicates the energy at which the stripping model predicts product dissociation to be complete (see text).

The present uranium ion source is the result of substantial experimentation with surface ionization sources. The techniques of vaporizing uranium metal and ionizing by electron impact or surface ionization did not yield sufficiently high ion currents and presented materials problems. Uranyl salts deposited directly on rhenium ribbons exhibited the problem of oxide contaminants in the ion beam, since uranium monoxide and dioxide have lower ionization potentials than the metal.^{9,23} This problem also necessitated the careful elimination of sources of oxygen, including water due to outgassing, in the vicinity of the hot filament.

III. RESULTS AND DISCUSSION

A. Reaction of U^+ with N_2

Uranium ions react with nitrogen molecules to yield UN^* , Eq. (9). Variation of cross section with relative translational energy is shown in Fig. 3. Absolute cross sections are calculated using

$$I_p = (I_p + I_{U^+})(1 - e^{-nQl}), \quad (11)$$

which relates the cross section Q , the length of the interaction region l , and the density of the target gas n to the measured reactant and product ion beam intensities I_{U^+} and I_p , respectively.

In ion beam-collision chamber experiments, significant Doppler broadening of relative collision energies results from thermal motion of the target gas. Using the analysis of Chantry²⁵ for a cross section which increases linearly with energy above threshold, an extrapolation of the straight line portion of the curve gives

a threshold too low by $3\gamma kT$, where T is the temperature of the target gas and $\gamma = m_U / (m_U + m_{AB})$, m_U and m_{AB} being the incident particle and target gas masses. The extrapolated threshold (the dashed line in Fig. 3) is 5.0 ± 0.2 eV, which when corrected becomes 5.1 ± 0.2 eV. Chantry gives the full width at half-maximum of the relative kinetic energy distribution

$$W_{1/2} = (11.1 \gamma k T E)^{1/2} \quad (12)$$

at an energy E . For Reaction (9) with $E = 5.1$ eV, $W_{1/2}$ is 1.3 eV. In accordance with Chantry's analysis, this is approximately the difference between the observed onset of reaction and the corrected threshold.

The threshold obtained for Reaction (9) yields a bond dissociation energy of 4.7 ± 0.2 eV for UN^* dissociating to ground state U^* and N . Other data used in this calculation are summarized in Table I. The heat of formation of UN^* is calculated to be 272 ± 7 kcal/mole. The major uncertainty in this figure is the poorly known heat of formation for the uranium atom.

The behavior of the cross section at energies above threshold can be explained by examining the deposition of energy during reaction. Dissociation of the product ion UA^* can first occur at the threshold for the reaction



This energy is merely the bond dissociation energy of AB . For Reaction (9), $D(N_2) = 9.80$ eV, this is the approximate point (marked by an arrow in Fig. 3) at which the cross section ceases to rise linearly and begins to decrease with increasing energy. The stripping model,^{21,26} which requires that no momentum be transferred to the neutral product B during reaction, constrains the internal energy of the product UA^* to be

$$E_{int} = \frac{m_A(m_{AB} + m_U)}{m_{UA}m_{AB}} E - E_T, \quad (14)$$

TABLE I. Thermochemical data.

Species	$\Delta H_f^\circ, 298$ (kcal/mole)	Reference
U	125 ± 5	a
U^+	268 ± 5	a, b
H^+	367.19 ± 0.01	c
	D_{298}° (kcal/mole)	
N-N	226 ± 2	c
D-D	106 ± 0.1	d
D- CD_3	104.9 ± 0.05	d
U-N	126 ± 5	e
$U^+ - N$	108 ± 5	This work
$U^+ - H$	67 ± 5	This work

^aS. D. Gabelnick, "Ion Reactor Safety and Physical Property Studies," Annual Report, July 1973-June 1974, Chemical Engineering Division, Argonne National Laboratory, ANL-8120).

^bCalculated from $\Delta H_f^\circ(U)$ and $I. P. (U) = 6.187 \pm 0.002$ eV given in Ref. 1.

^cJANAF Thermochemical Tables, Natl. Stand. Ref. Data Ser. Natl. Bur. Stand. 37 (1971).

^dD. deB. Darwent, Natl. Stand. Ref. Data Ser. Natl. Bur. Stand. 31 (1970).

^eData from Ref. 12.

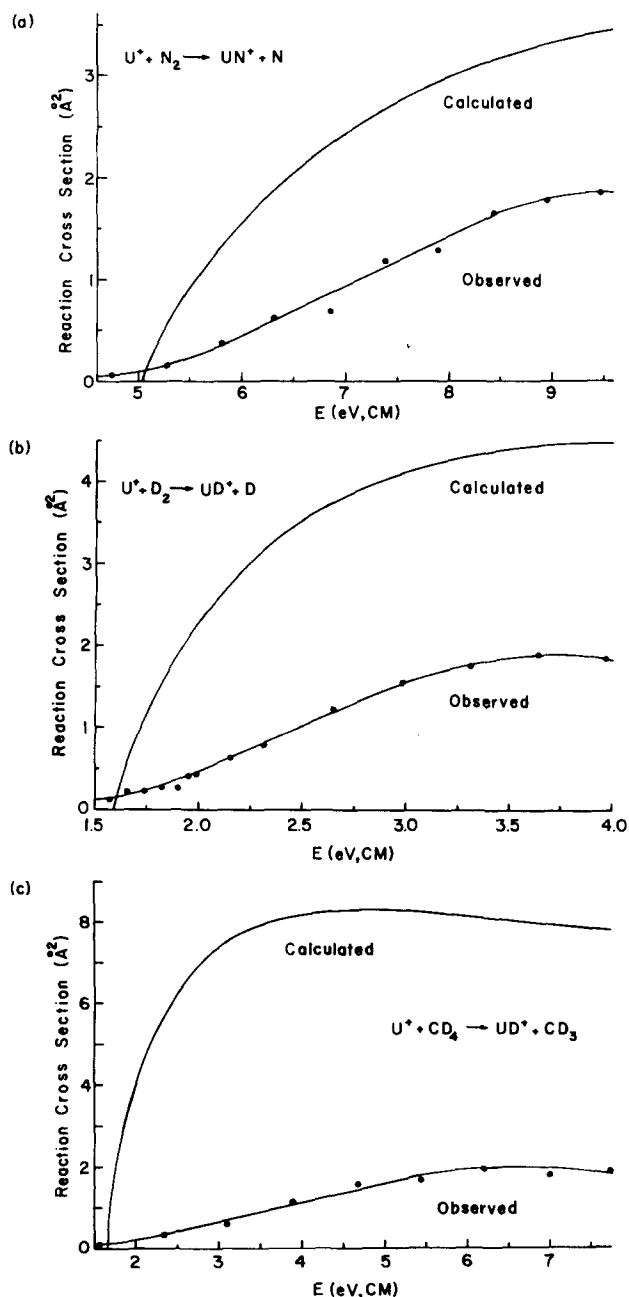


FIG. 4. A comparison of the cross section predicted by Eq. (18) to experimental results for (a) Reaction (9), (b) Reaction (19), and (c) Reaction (21).

where E_T , the threshold for reaction, equals $D(AB) - D(UA^*)$. Since dissociation occurs when $E_{int} = D(UA^*)$, the energy at which the stripping model predicts dissociation should be complete is

$$E_s = \frac{m_U m_{AB}}{m_A(m_{AB} + m_U)} D(AB). \quad (15)$$

For the nitrogen reaction E_s equals 18.6 eV. The experimental cross section, Fig. 3, decreases up to this point, above which it has a small and approximately constant value of $\sim 0.1 \text{ \AA}^2$. The persistent cross section at high energy could easily result from reaction at small impact parameters with appreciable momentum transfer to the neutral product.

At low energies the long range interaction between an ion and a nonpolar neutral molecule is given by

$$V(r) = -\alpha e^2 / 2r^4, \quad (16)$$

where α is the angle averaged polarizability of the neutral and r is the reactant separation. The motion under the influence of this long range interaction is such that the cross section for close encounters is given by

$$Q_i = \pi e (2\alpha/E)^{1/2}, \quad (17)$$

where E is the relative kinetic energy. A simple model for endothermic reactions requires the kinetic energy along the line of centers to exceed E_T .²⁷ Equation (17) becomes modified by inclusion of the factor $(1 - E_T/E)$, giving

$$Q_i = \pi e (2\alpha/E)^{1/2} (1 - E_T/E). \quad (18)$$

Figure 4(a) compares the cross section of Eq. (18) to the experimental cross section in the threshold region. If the model leading to Eq. (18) is presumed correct, Reaction (9) proceeds with a reaction efficiency of approximately 50%. It is noted, however, that the orbiting impact parameter calculated at threshold (1.8 Å at 5.1 eV) is roughly equal to the molecule separation expected for a hard sphere interaction.

B. Reaction of U^+ with D_2

Experimental results for the reaction of uranium ions with deuterium



are shown in Fig. 5. The corrected threshold is $1.7 \pm 0.1 \text{ eV}$ with $W_{1/2} = 0.8 \text{ eV}$ at this energy. Again the

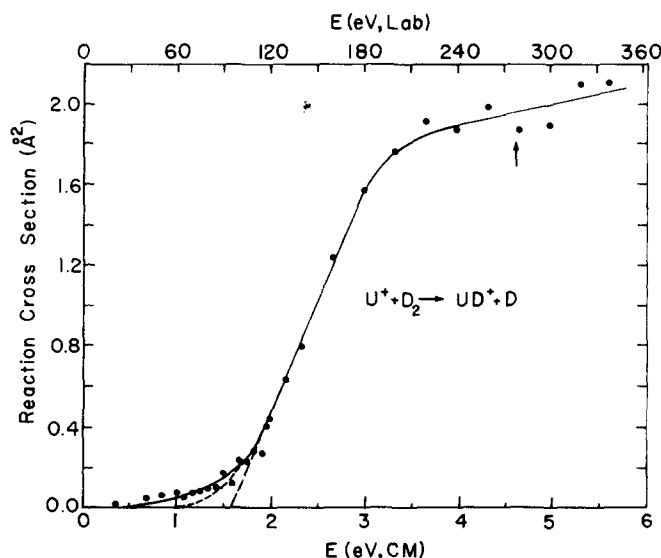


FIG. 5. Variation of experimental cross section with relative kinetic energy in the center of mass frame (lower scale) and the laboratory frame (upper scale) for Reaction (19). The solid curve is an approximate fit to the experimental points. The straight dashed line (---) is a linear extrapolation of the data in the threshold region. The curved dashed line (---) is the threshold behavior predicted by Chantry's analysis at a temperature of 400°K. The arrow at 4.6 eV indicates the threshold for the product channel $U^+ + D + D$.

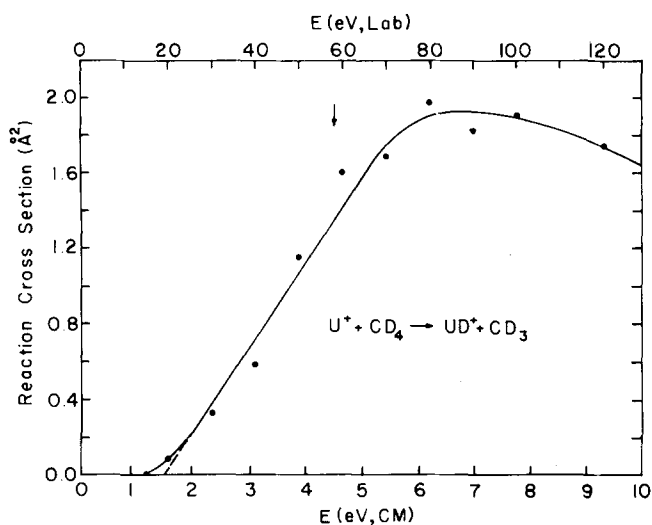


FIG. 6. Variation of experimental cross section with relative kinetic energy in the center of mass frame (lower scale) and the laboratory frame (upper scale) for Reaction (21). The solid curve is an approximate fit to the experimental points. The straight dashed line (—) is a linear extrapolation of the data in the threshold region. The threshold behavior predicted by Chantry's analysis at 400°K is coincident with the solid curve. The arrow at 4.6 eV indicates the threshold for the product channel $U^+ + D + CD_3$.

apparent onset is lower than the corrected threshold by approximately $W_{1/2}$. The bond dissociation energy for UD^+ is 2.9 ± 0.1 eV and the derived heat of formation is 254 ± 6 kcal/mole.

The dissociation process



becomes energetically feasible at 4.6 eV. The cross section levels off at a somewhat lower energy, 3.5 eV. The energy at which dissociation should be complete according to the stripping model is 9.1 eV, which is considerably higher than the range of energies accessible in the present experiment. The reaction efficiency by the polarization theory, Fig. 4(b), is approximately 40%.

C. Reaction of U^+ and CD_4

The threshold for the reaction



provides a check of the thermodynamic data derived from the reaction with deuterium. The variation of reaction cross section with relative kinetic energy is shown in Fig. 6. The corrected threshold, 1.6 ± 0.3 eV, leads to $\Delta H_f(UD^+) = 252 \pm 8$ kcal/mole, in excellent agreement with the previous experiment. This corresponds to a bond dissociation energy of 3.0 ± 0.3 eV for the UD^+ ion.

Consideration of the energy deposition in Reaction (21) is rendered difficult by the internal degrees of freedom in the polyatomic neutral product. Interestingly, the cross section levels off in the region of the lowest energy dissociation process, at $E = D(CD_3 - D) = 4.6$ eV. Again the dissociation energy predicted by

the stripping model, 42.3 eV, is beyond the energies examined in the present experiment. Figure 4(c) suggests the reaction efficiency is near 25%.

IV. CONCLUSION

As originally suggested by Johnsen and Biondi,¹⁸ Reaction (9) is endothermic. The highest relative kinetic energy in their experiments, 0.53 eV, is considerably below the 5.1 eV threshold observed in the present experiment. The estimate of Moreland, Rokop, and Stevens¹⁷ for $D(UD^+)$, 3.3 ± 0.5 eV, agrees with the values of 2.9 ± 0.1 and 3.0 ± 0.3 eV within experimental accuracy.

The present experiments arrive at the bond dissociation energies $D(UN^+) = 4.7 \pm 0.2$ and $D(UH^+) = 2.9 \pm 0.2$ eV.²⁸ Using these data and $I.P.(U) = 6.187 \pm 0.002$ eV,¹ it is seen with reference to Fig. 1 and Eq. (3) that the general chemi-ionization reaction (2) is endothermic for $A = N$ and H . The endothermicity

$$\Delta H = I.P.(U) - D(UA^+) = I.P.(UA) - D(UA) \quad (22)$$

is 1.5 eV for the nitrogen reaction and 3.3 eV for hydrogen. From the bond dissociation energy of neutral uranium nitride $D(UN) = 5.5 \pm 0.2$ eV,^{12(a)} the ionization potential of UN is calculated to be 7.0 ± 0.3 eV. Ginterich has estimated using electron impact ionization that $I.P.(UN)$ is approximately 1 eV higher than $I.P.(U)$, giving a value of 7.2 eV, which is in good agreement with our result. The reactions of nitrogen and hydrogen atoms contrast with those of oxygen and sulfur atoms, where process (2) has been observed to be exothermic.^{7(c),(d)} The difference in energetics between the oxygen and nitrogen systems is shown explicitly in Fig. 7. In multiple photon uranium atom ionization experiments isotope selective excitation of the 5K_6 level at 2.05 eV has been demonstrated.² Sufficient energy is available in this state for Reaction (2) to be exothermic with nitrogen but not hydrogen atoms.

It is of interest to calculate the proton affinity of the uranium atom using the relationship²⁹

$$P.A.(U) = D(UH^+) + I.P.(H) - I.P.(U) \quad (23)$$

The value derived, 238 ± 5 kcal/mole, is compared with the proton affinities of selected atomic and molecular species in Table II. Within this broad range of base

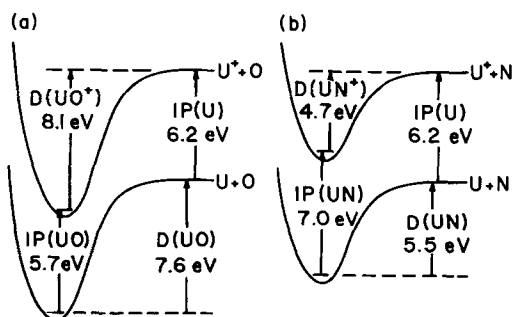


FIG. 7. A comparison of the energetics for the associative ionization reaction of ground state uranium atoms with (a) oxygen atoms and (b) nitrogen atoms.

TABLE II. Proton affinities of selected atomic and molecular species.

Species	Ionization potential (eV)	Proton affinity (kcal/mole)	Reference for proton affinities
Li	5.39 ^e	193 ± 5	a, b
Mg	7.64 ^e	187 ± 5	b, d
Hg	10.44 ^e	128 ± 5	b, d
U	6.19 ^f	238 ± 5	This work
NMe ₃	7.87 ^g	222 ± 2	g
PMe ₃	8.01 ^g	224 ± 2	g
NEt ₃	7.42 ^h	229 ± 2	c
LiOH		241 ± 2	i
NaOH		248 ± 2	i
KOH		263 ± 2	i
CsOH		270 ± 2	i

^aF. H. Field, Natl. Stand. Ref. Data Ser. Natl. Bur. Stand. 26, (1969).

^bJANAF thermochemical tables, Natl. Stand. Ref. Data Ser. Natl. Bur. Stand. 37 (1971).

^cJ. F. Wolf, R. H. Staley, I. Koppel, M. Taagepera, R. T. McIver, Jr., J. L. Beauchamp, and R. W. Taft, *J. Am. Chem. Soc.* (submitted for publication).

^dG. Herzberg, *Spectra of Diatomic Molecules* (Van Nostrand, New York, 1965), Table 39.

^eB. Lakatos, J. Bohus, and G. Medgyesi, *Acta. Chim. Hung.* 20, 1 (1959).

^fReference 1.

^gR. V. Hodges and J. L. Beauchamp, *J. Inorg. Chem.* 14, 2887 (1975).

^hR. H. Staley, M. Taagepera, W. G. Henderson, J. L. Beauchamp, and R. W. Taft, *J. Am. Chem. Soc.* 99, 326 (1977).

ⁱS. K. Searles, I. Dzidic, and P. Kebarle, *J. Am. Chem. Soc.* 91, 2810 (1969).

strengths uranium clearly emerges as the most basic of all atoms for which reasonable thermochemical data are available. Uranium atoms are more basic than the strongest organic monodentate bases. Only the alkali hydroxides appear to be more basic. The high base strength of uranium results from the combination of a strong homolytic bond dissociation energy and a low ionization potential. The methodology developed in the present investigation can be generally applied to determine metal base strengths and metal hydrogen homolytic bond dissociation energies.

ACKNOWLEDGMENTS

This work was supported in part by the Ford Motor Company Fund for Energy Research administered by the California Institute of Technology and by the Energy Research and Development Administration.

*Camille and Henry Dreyfus Teacher-Scholar, 1971-1976.

¹G. S. Jones, I. Itzan, C. T. Pike, R. H. Levy, and L.

Levin, *J. Quantum Electron QE-12*, 111 (1976).

²L. R. Carlson, J. A. Paisner, E. F. Warden, S. A. Johnson, C. A. May, and R. W. Solary, *J. Opt. Soc. Am.* 66, 846 (1976).

³J. P. M. Schmitt, *Bull. Am. Phys. Soc.* 21, 1042 (1976), Abstract 1P4.

⁴J. M. Dawson, H. C. Kim, D. Arnush, B. D. Fried, R. W. Gould, L. O. Heflinger, C. F. Kennel, T. E. Romesser, R. L. Stenzel, A. Y. Wong, and R. F. Wuerker, *Phys. Rev. Lett.* 37, 1547 (1976).

⁵S. Wexler *et al.* Abstracts of papers, 172nd ACS Natl. Meeting, San Francisco, CA, 29 Aug.-3 Sept., 1976.

⁶F. Devienne (unpublished results).

⁷(a) W. L. Fite, H. H. Lo, and P. Vasu, Abstracts, IXth International Conference on the Physics of Electronic and Atomic Collisions, Seattle, 24-30 July 1975; (b) M. W. Siegel and W. L. Fite, *ibid.*; (c) W. L. Fite, H. H. Lo, and P. Irving, *J. Chem. Phys.* 60, 1236 (1974); (d) W. L. Fite (private communication).

⁸M. H. Rand and O. Kubaschewski, *Thermochemical Properties of Uranium Compounds* (Oliver and Boyd, London, 1973).

⁹E. G. Rauh and R. J. Ackermann, *J. Chem. Phys.* 60, 1396 (1974).

¹⁰E. D. Cater, P. W. Gilles, and R. J. Thorn, *J. Chem. Phys.* 35, 608 (1961); E. D. Cater, E. G. Rauh, and R. J. Thorn, *ibid.* 35, 619 (1961); 44, 3106 (1966).

¹¹D. L. Hildenbrand, Stanford Research Institute, Project No. PYU 4822, 7 June, 1976.

¹²(a) K. A. Gingerich, *J. Chem. Phys.* 47, 2192 (1967); (b) 50, 2255 (1969); (c) 53, 746 (1970).

¹³R. N. Compton, *J. Chem. Phys.* 66, xxx (1977).

¹⁴J. L. Beauchamp, *J. Chem. Phys.* 64, 718 (1976); 64, 929 (1976).

¹⁵N. A. McAskill, *Aust. J. Chem.* 28, 1879 (1975).

¹⁶C. E. Young, P. M. Dehmer, R. B. Cohen, L. G. Paba, and S. Wexler, *J. Chem. Phys.* 64, 306 (1976).

¹⁷P. E. Moreland, D. J. Rokop, and C. M. Stevens, *Int. J. Mass Spectrom. Ion Phys.* 5, 127 (1970).

¹⁸R. Johnsen and M. A. Biondi, *J. Chem. Phys.* 57, 1975 (1972).

¹⁹R. V. Hodges and J. L. Beauchamp, *Anal. Chem.* 48, 825 (1976).

²⁰H. W. Werner, *Int. J. Mass Spectrom. Ion Phys.* 14, 189 (1974).

²¹Z. Herman and R. Wolfgang, *Ion-Molecule Reactions*, edited by J. L. Franklin, (Plenum, New York, 1972), p. 553.

²²G. R. Hertel, *J. Chem. Phys.* 47, 133 (1967).

²³J. B. Mann, *J. Chem. Phys.* 40, 1632 (1964).

²⁴E. W. Rothe, *J. Vacuum Sci. Tech.* 1, 66 (1964).

²⁵P. J. Chantry, *J. Chem. Phys.* 55, 2746 (1971).

²⁶A. Henglein, in *Ion Molecule Reactions in the Gas Phase*, edited by Pierre Ausloos (ACS, Washington, D.C., 1966), p. 63.

²⁷R. D. Levine and R. B. Bernstein, *Molecular Reaction Dynamics* (Oxford University, New York, 1974), p. 46.

²⁸The substitution of protium (H) for deuterium (D) in the following discussion is made at this point. We estimate that the difference in bond dissociation energies for the two isotopes is 1.7 kcal/mole, leading to the value $D(UH^+) = 2.9 \pm 0.2$ eV.

²⁹J. L. Beauchamp, *Ann. Rev. Phys. Chem.* 22, 527 (1971).